

# 特集 | コンベ車向け機械式回生発電システムの省燃費効果 定量化\*

## Fuel Economy Analysis of Alternator with Kinetic Energy Storage for a Conventional Vehicle

田中 栄太郎  
Eitaro TANAKA

成田 隆大  
Takahiro NARITA

前川 仁之  
Hitoshi MAEGAWA

This paper evaluates the effect of our new alternator concept for a conventional vehicle, which is able to generate electricity by storing kinetic energy of the vehicle in the high flywheel as rotation energy under deceleration. The alternator constructs a planetary gear device and multiple clutch-brakes perform CVT, alternator and high speed flywheel without an expensive electric device, mechanical CVT and vacuum pump. So it has high cost performance.

Key words : Alternator, generate electricity, kinetic energy, flywheel, fuel economy

### 1. INTRODUCTION

Fuel economy regulations have been increasingly tight due to, among other things, global warming and soaring crude oil prices. Europe, which has the strictest regulations, requires CO<sub>2</sub> emissions to be reduced by 30% from 2011 levels by 2020 and afterward (see Fig. 1). This trend is expected to accelerate since energy demand will rise each year based on future population increases and growth of emerging economies. To meet the fuel economy regulations, vehicle electrification has been expanding, as seen with HVs and EVs. However, it is forecast that internal combustion engine (ICE) vehicles (especially compact cars) will remain dominant even in 2020 (see Fig. 2) because of such problems that include expensive HV and EV prices and infrastructure deployment. Consequently, it is necessary to improve the fuel efficiency of compact ICE cars, which will remain the mainstream. However, since integration of existing fuel-saving technologies currently studied in the world is, on its own, not enough, it is vital that additional measures are devised.

In the search for measures to improve the fuel efficiency of ICE cars, the current state was analyzed through measurement of the energy balance in actual ICE vehicles. Fig. 3 shows the energy balance for a range encompassing from the heat value of the gasoline up to the driving of the wheels in Japanese in-use fuel economy mode. Fuel economy improvement perspectives

were identified according to the magnitude of energy lost, including ① Improvements in engine thermal efficiency, ② Improvement in power transmission, ③ Waste heat recovery, ④ Reductions in auxiliary losses, and ⑤ Braking energy recovery. Among these factors, ① through ④ have seen technological development to the point where there are few feasible improvements left. In contrast, ⑤ braking energy recovery was assessed as promising for the following reasons.

- (1) ⑤ generates a larger amount of energy than ② or ④. Braking during deceleration dissipates 1.5 MJ, sufficient energy to drive the alternator, which requires 1.2 MJ.
- (2) ⑤ provides better quality energy than ③. Since ⑤ generates power in the form of torque multiplied by rotational speed, the system configuration would highly probably be simple and with low losses.

Electricity requirements and braking energy of a B-segment car were measured to identify problems in regenerating braking energy and using it as electricity. Regarding auxiliaries, only the air-conditioning system was operated during the test. The navigation, proximity sensor, rear view camera, and EPS systems were not operated. Fig. 4 shows a time-series graph of braking energy and electricity requirements in the in-use fuel economy mode drive cycle. The graph reveals that the total electricity requirements of the vehicle amount to 680 kJ, which is about one half of the total braking energy (1420 kJ). Meanwhile, electricity con-

\* Reprinted with permission from SAE paper 2013-01-0481 © 2013 SAE International.  
Further use or distribution of this material is not permitted without permission from SAE.

sumption is constantly 0.35 kW (on average), while braking energy of 3.4 kW (on average) is generated intermittently. In other words, although the braking energy meets the electricity requirements in terms of the total amount of energy, it does not continuously cover the requirements. Moreover, the current on-board lead acid battery has a low maximum input capacity of a few hundred watts, resulting in regeneration of only a fraction of the braking energy. Consequently, to use braking energy as electricity, it is necessary to use an energy storage device that temporarily stores a large amount of energy.

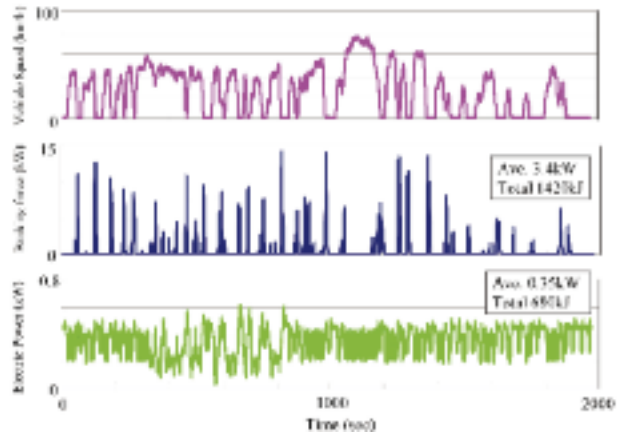


Fig. 4 Braking energy and electrical power in in-use fuel economy cycle

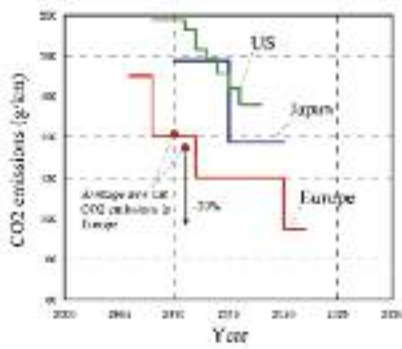


Fig. 1 CO2 emissions standard

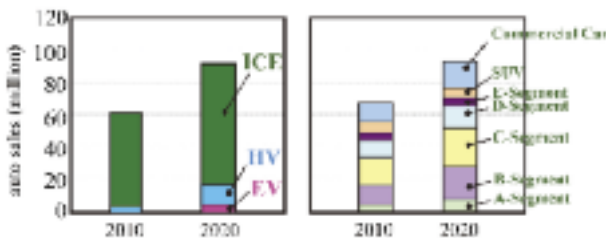


Fig. 2 Automotive Powertrain & Segment Outlook

Table 1 Comparison of energy storage methods

Form of Energy	Electricity	Pressure	Kinetic Energy
Example	Battery (Li-Ion) Ultra Capacitor	Accumulator	High Speed Flywheel
Self Discharge Rate	1 %/Year	5 %/Month	2 %/min
Specific Power Density	0.5 kW/kg	2 kW/kg	1.2 kW/kg
Durability	1,000 Cycles	100,000 Cycles	Semi-permanent
Operating Temperature Range	0-60	-35-70	-55-80
Understanding, Charging Cycle	easy	needs technology	needs special technology
Maintainability	easy to maintain	needs special maintenance	needs special maintenance
Cost	high cost (2012) but decreasing	expensive	expensive

電省  
動工  
化ネ

Energy storage devices currently considered promising are categorized into three types according to energy storage form (Table 1): power generated by a generator and stored as electricity; fluid pressure increased by a pump or the like and stored as pressure; and the speed of a rotating body of significant inertial mass increased by reduction gear or the like and stored as kinetic energy. These present their respec-

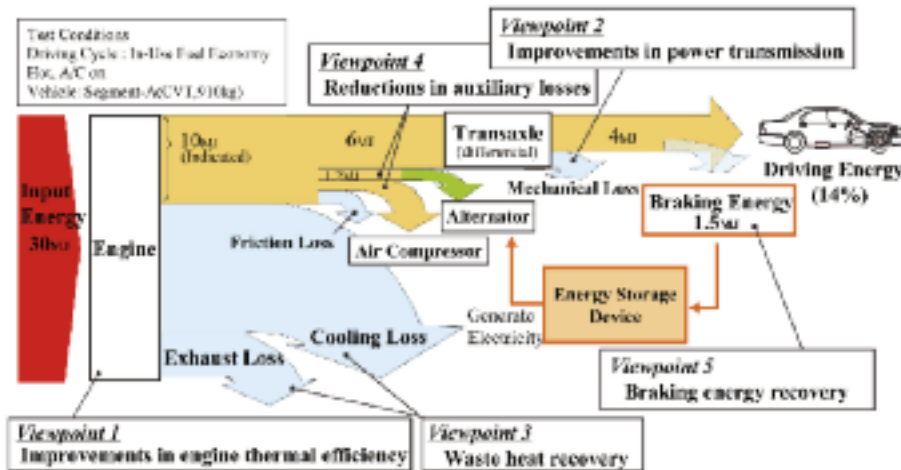


Fig. 3 Energy flow in conventional vehicle

tive challenges in implementation. Efforts are underway to meet these challenges. Flywheel (FW) systems fall into types that store energy as kinetic energy. Compared with other devices, the FW system has the following advantages:

- Changes in characteristics caused by ambient temperature changes are small plus excellent durability since the system is entirely composed of mechanical parts
- High cost reduction potential since no minor metals are used
- Can be highly efficient due to the absence of energy conversion
- Handles large amounts of energy with ease since the maximum input is determined largely by mechanical parts such as gears and bearings

The FW system is considered promising for use in conventional vehicles specifically due to few restrictive conditions (temperature and durability) in application and cost reduction potential. We have designed a system, combining an existing alternator and an FW, to temporarily store a large amount of braking energy as rotational energy in the FW and to operate the alternator to generate power when electricity is needed. For installation in mass-produced vehicles, however, it was necessary to address challenges such as simplified reduction gear and generator designs, avoiding the use of a vacuum pump, and use of a low-cost FW material. This paper details these challenges and presents ideas as solutions to them.

## 2. CONCEPT OF AN ALTERNATOR WITH KINETIC ENERGY STORAGE

### Challenges

#### 1. Simplified Reduction Gear and Generator Designs

Storing energy in a FW system increases the FW speed. To this end, it is necessary to change the rotational speed on the part of the vehicle to a higher speed than the FW speed with a device that provides continuous speed variation. The following three systems are used for continuous speed variation. High cost is an issue with all these systems because of the need for expensive equipment such as CVT and motor inverter.

##### (i) Electrical conversion system:

Converts braking energy into electrical energy via a generator. The electrical energy is used to increase the speed of a motor coupled to a FW to store the energy. For power gen-

eration, the motor coupled to the FW is used as a generator.

##### (ii) CVT system:

The input shaft on the vehicle is coupled to the input shaft of a toroidal or belted continuously variable transmission. The output shaft is coupled to a FW. This system changes the speed input from the vehicle to increase the FW speed. For power generation, a generator coupled to the FW is used.

##### (iii) Electric CVT system (Prius THS system):

Three shafts of planetary gear are used as an input shaft (input shaft on vehicle), output shaft (coupled to the FW), and speed change shaft (coupled to the motor) to change the speed input from the vehicle to increase the FW speed. Power is generated by a motor inverter coupled to the speed change shaft.

### 2. Avoiding the Use of a Vacuum Pump

At high FW speeds, losses (windage losses) are produced by friction between the FW and the air. The magnitude of the loss is roughly proportional to the ambient pressure. In some cases with our competitors, this problem is addressed by installing a vacuum pump, which is costly.

### 3. Use of a Low-Cost FW Material

Flywheels rotating at high speeds are associated with a failure mode involving breakage caused by the centrifugal force. Centrifugal forces are determined by the following equation:

$F = m r \omega^2$  ( $m$ : mass;  $\omega$ : rotational speed). The amount of stored energy is determined by the following equation:

$E = 1/2 I \omega^2$  ( $I$ : moment of inertia  $\approx m$ ;  $\omega$ : rotational speed).

Consequently, the use of a light and low-speed FW with the aim of increasing the material strength reduces the amount of stored energy and translates to reduced effectiveness of the FW in improving the fuel economy. One solution to this tradeoff is the use, at high speeds, of a high specific strength material (CFRP or magnesium alloy) that has a high strength to weight ratio. However, this solution is costly.

### Solutions

Our solutions to these challenges are shown in **Fig. 5**. To reduce the cost, this system incorporates an electric CVT, the already installed alternator as motor coupled to the speed change shaft, negative engine pressure (intake) instead of a vacuum pump, and a FW constructed of steel. The system has three components, which work as explained below.

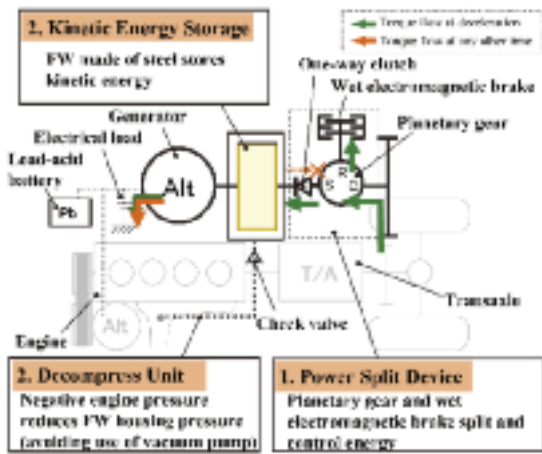


Fig. 5 Schematic of the Alternator with Kinetic Energy Storage

1. Power Split Device: planetary gear (simplified reduction gear and generator designs)

Provides functions to change the axle rotational speed to match the FW speed. In the present system, the carrier, sun gear, and ring gear are used respectively as input shaft, output shaft, and speed change shaft. The ring gear and the wet electromagnetic brake are coupled. The braking torque of the wet electromagnetic brake controls the torque transmitted to the ring gear to continuously change the gear ratio between the input and output shafts. Since a wet electromagnetic brake is used to provide control instead of an expensive motor inverter, control works only in the direction of ring gear deceleration, imposing limitations on the speed change range. The system has this disadvantage, but its cost can be reduced. Moreover, a one-way clutch is installed between the sun gear and energy storage to avoid losses in the stored energy.

2. Decompress Unit: non-vacuum/decompression piping (avoiding the use of a vacuum pump)

Decompresses the FW housing with negative engine pressure (intake), providing functions to reduce losses caused by FW rotating at high speeds. Since the negative engine pressure is expected to reduce the pressure to 20 to 30 kPa, windage losses diminish to one-fourth to one-fifth of those that would occur in the atmosphere. Although the present system has greater windage losses than in a vacuum (windage loss: 0 W), the design avoids the use of a vacuum pump and offers optimum FW geometry and housing to reduce the cost.

3. Kinetic Energy Storage: FW (low-cost FW)

Provides functions to store energy as FW rotational force. The system uses a FW made of steel and limits its maximum speed so that the material strength is not exceeded. Although the system speed will be lower than achievable with a high specific strength material (e.g., CFRP), a higher-density material (steel) is advantageous since the surface area of the FW will be smaller for the same inertia, given operations in a non-vacuum, or under low pressure conditions. Furthermore, the cost is expected to be low.

Power Split Device

The system achieves regenerative braking, as explained below.

1. During Deceleration (Fig. 6, Fig. 7)

① In response to the driver's request for braking, torque output to the wet electromagnetic brake is multiplied by a factor of the gear ratio of the planetary gear and applied to the ring gear of the planetary gear. Rotative power is transferred from the vehicle to the carrier, sun gear and to the FW, increasing the FW speed to store energy.

② Total torque applied to the ring gear and sun gear is applied to the axle as braking torque and the vehicle decelerates.

③ Energy stored by the FW is converted into electricity by the alternator coupled to the FW.

In this process, the three shafts of the planetary gear undergo changes, as shown in the collinear diagram (Fig. 7).

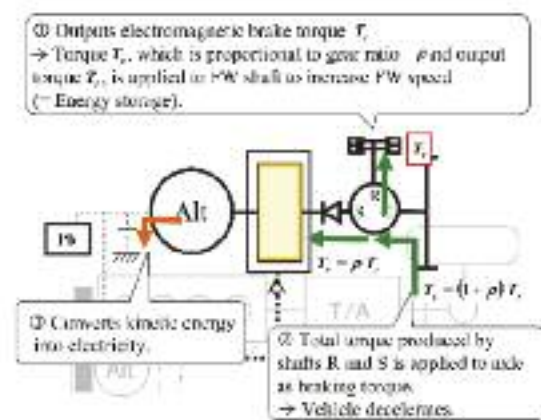


Fig. 6 Routine of storing kinetic energy of the vehicle under deceleration

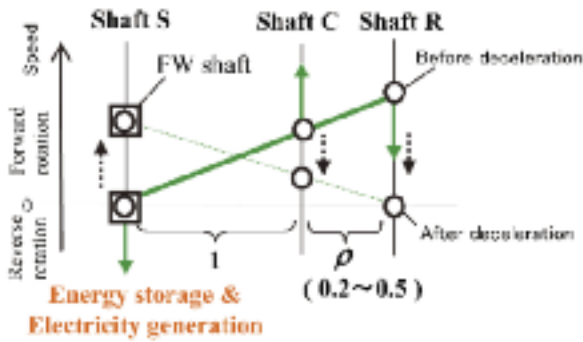


Fig. 7 Collinear diagram of planetary gear under deceleration

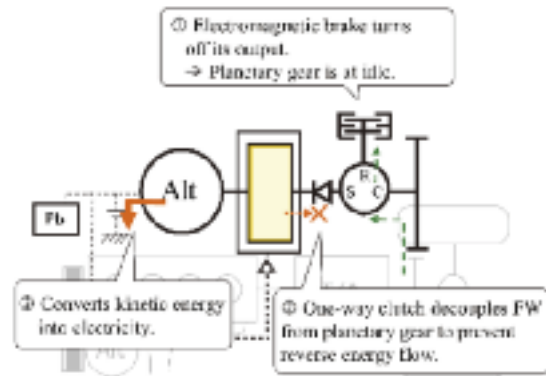


Fig. 8 Routine of generating electric energy from stored kinetic energy under constant-velocity drive, acceleration and stopping

2. Acceleration, Constant-Velocity Drive, and Stopping (Fig. 8, Fig. 9)

- ① The electromagnetic brake turns its output off. The ring gear of the planetary gear is at idle.
- ② The one-way clutch installed between the sun gear and energy storage prevents stored energy from flowing back to the planetary gear.
- ③ The alternator coupled to the FW converts kinetic energy stored by the FW into electricity for use when needed.

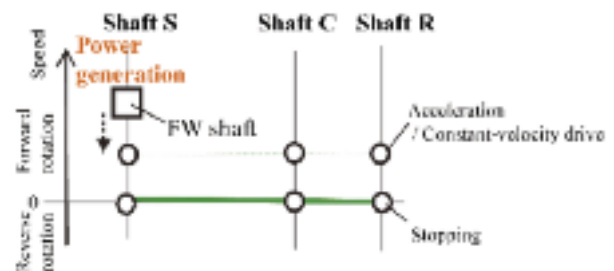


Fig. 9 Collinear diagram of planetary gear under constant-velocity drive, acceleration and stopping

Flywheel Material

Steel (SCM415) was selected as FW material to provide anticipated cost reduction, as has been discussed. Fig. 10 shows losses caused by the FW determined through a calculation. The amount of stored energy was 150 kJ. The operating pressure was 20 kPa. Regarding rotor geometry (aspect

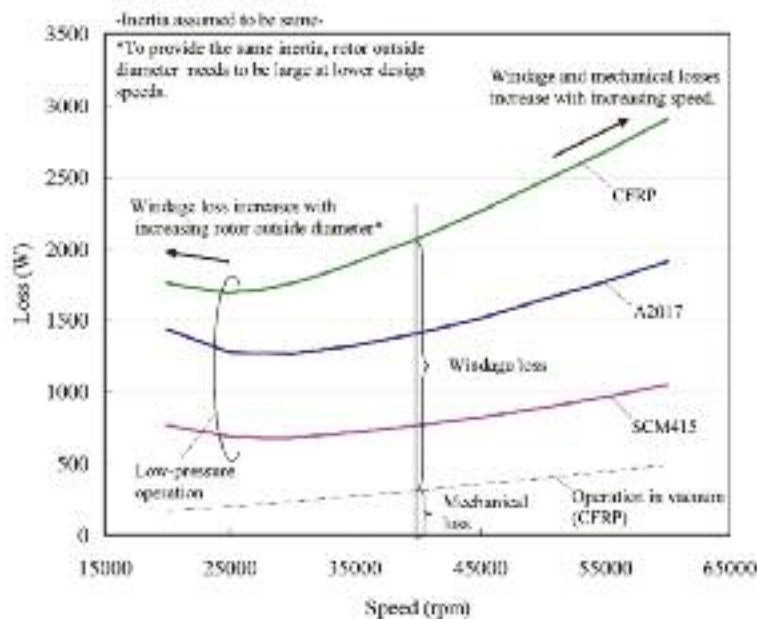


Fig. 10 Rotational loss in flywheel

ratio), the outside diameter was selected according to the upper limit, which was the maximum permissible circumferential speed (fracture velocity) of each rotor material or the speed of sound, whichever was lower, so as to minimize the weight (see Equation (1)).

$$E = \frac{1}{2} I_{fw} \omega^2 = \frac{1}{4} \rho_{fw} \pi r^2 e \omega^2 \dots (1)$$

where, E: amount of stored energy (kJ);  $I_{fw}$ : moment of inertia of FW ( $\text{kgm}^2$ );  $\omega$ : FW speed (1/s);  $\rho_{fw}$ : density ( $\text{kg/m}^3$ );  $r$ : FW radius (m); and  $e$ : FW thickness (m).

The trial calculation was performed on the three rotor material types of CFRP, aluminum (A2017), and steel (SCM415). Primary losses associated with FW rotation, including windage, seal, gear, and bearing losses, were calculated by the following empirical Equations (2) through (5).

Windage loss <sup>1)2)3)</sup>:  $L = \frac{k}{8} \rho r^4 (2r + 5e) \omega_{fw}^3 \dots (2)$

(An equation for rotating disks is shown since no equations exist for rotating cylinders.)

Seal loss:  $L = T_{ref} (\omega_s / \omega_{ref})^{1.1} \omega_s \dots (3)$

Gear losses <sup>4)</sup>: Oil stirring loss ...,  $L = 0.368 \times 10^{-3} b y v^{1.5} \dots$

Engagement loss ...  $L = \frac{\mu}{d \cos \alpha_n \cos \beta} \cdot \frac{1+i}{i} \cdot \frac{l_a^2 + l_r^2}{l_a + l_r} \dots (4)$

Bearing loss <sup>5)</sup>:  $L = 0.672 \times 10^{-6} D^{0.5} F^{1.1} \omega_b$   
 $+ 3.47 \times 10^{-3} D^{0.5} n^{1.1} Z^{0.4} Q^{0.12} v^{0.2} \omega_b \dots (5)$

where, k: coefficient of friction (-);  $\rho$ : air density ( $\text{kg/m}^3$ );  $r$ : FW radius (mm);  $e$ : FW thickness (mm);  $\omega_{fw}$ : FW speed (1/s);  $\omega_{ref}$ : typical speed (1/s);  $T_{ref}$ : torque loss when speed of seal sliding section is  $\omega_{ref}$ ;  $\omega$ : speed of seal sliding section (1/s);  $b$ : gear face width (mm);  $y$ : oil immersion depth of gear (mm);  $v$ : circumferential speed of gear (m/s);  $\mu$ : mean coefficient of friction of gear (-);  $d$ : gear pitch circle diameter (mm);  $\alpha_n$ : normal pressure angle ( $^\circ$ );  $\beta$ : helix angle ( $^\circ$ );  $i$ : gear ratio (-);  $l_a$ : length of approach path (mm);  $l_r$ : length of recess path (mm);  $D$ : rotating body pitch diameter (mm);  $F$ : thrust load (N);  $n$ : bearing speed (rpm);  $Z$ : oil viscosity (cP);  $Q$ : lubrication rate (kg/min);  $\omega_b$ : bearing speed (1/s).

The figure reveals that CFRP that can rotate at higher speeds has advantages in a vacuum where the windage loss decreases to zero, while in low-pressure conditions subject to significant effects of windage loss, steel, being of high density, has advantages since its surface area can be smaller given the same inertia. Incidentally, losses are minimized in the range of 25000 to 28000 rpm and are greater in the lower speed range due to the need for a larger outside diameter and also greater in the higher speed range due to the effects of higher speeds.

**Specification**

Fig. 11 shows a conceptual drawing. To improve mountability, dead space was minimized: with the FW, alternator, and planetary gearing all coupled coaxially; bearings placed in the FW's inner space, since its contribution would be small; and the brake placed around the planetary gear. Functional parts were gathered and grouped for placement respectively in the atmosphere (alternator), low pressure (FW), and oil (reduction gear) to minimize shaft seals. The link between the system and the engine was used a conventional belt for installation in any vehicles, because it is a lot of flexibility in the design.

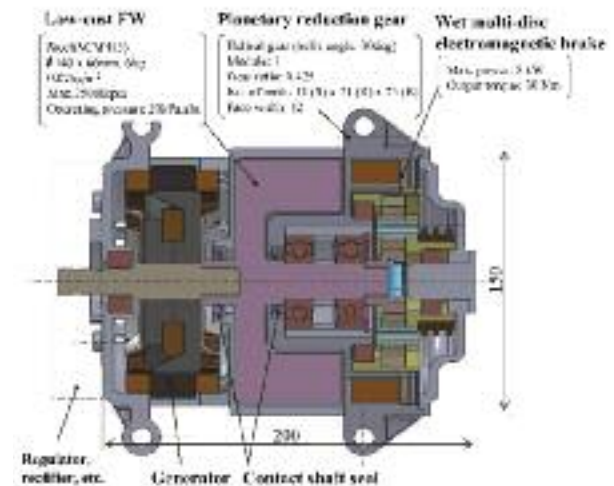


Fig. 11 Structural drawing of the alternator with kinetic energy storage

Table 2 shows the specifications. Parameters were set so as to maximize fuel economy improvement during the in-use fuel economy mode drive cycle <sup>2) 3) 4)</sup>.

電省  
動工  
化ネ

Table 2 Specifications

Parameter		Target	
System	Energy capacity	55kJ (18Wh)	
	Max. input	10kW	
	Max. output current	130A <small>(When cool, input voltage is constant at 0.5V)</small>	
	Max. braking force	1m/s <sup>2</sup>	
	Output response	max. 0.1sec	
	Continuous braking time	max. 50sec	
	Braking range	0-40km/h min. <small>(incl. 20km/h min. or average)</small>	
	Self Discharge rate	10%/min max.	
Energy storage	FW	Max. speed	25000rpm
		Inertia <small>(rotational inertia)</small>	0.2kg·m <sup>2</sup>
		Geometry	φ 140 x 66mm
		Operating pressure	20-40kPa, nbs <small>(Use of negative pressure (vacuum))</small>

### 3. SIMULATING IMPROVEMENTS IN FUEL CONSUMPTIONS

The effects of the system installed in a conventional compact car on fuel economy improvements were calculated based on the measurement data. Three drive modes were used: in-use fuel economy mode (Fig. 12); JC08 mode (Fig. 13); and NEDC mode (Fig. 14). In each drive mode, the driving force, indicated power of the engine, electrical load, fuel consumption, alternator efficiency, axle speed etc. of the vehicle were measured. Using these measurements, the braking force (regenerative energy), amount of generated electricity, and engine load (fuel consumption) reductions of the system brought about by the use of regenerative energy, were calculated on a time-series basis. The stored energy at the time of the run end was used to recharge the battery by the alternator. Table 3 shows the results.

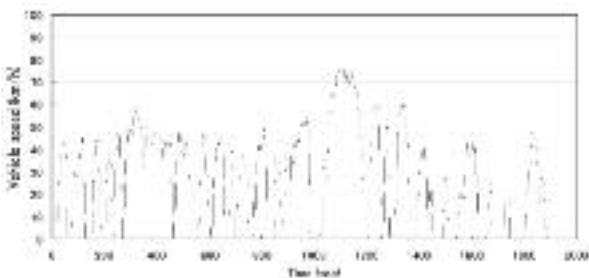


Fig. 12 In-use fuel economy mode drive cycle

Table 3 Fuel consumptions improvements

Cycle	Air Temperature	Humidity	Solar Radiation	Headlight	Start Condition	Air Conditioning (At 13/15 degrees)	
						On	Off
In-use Fuel Economy Mode	25 degrees	Not Cooled	None	Off	Hot	6.5%	8.0%
					Cool		
Japanese JC08 Mode	25 degrees	Not Cooled	None	Off	Hot	6.6%	8.0%
					Cool		
EURO	25 degrees	Not Cooled	None	Off	Hot	2.3%	
					Cool		
	25 degrees	Not Cooled	None	On	Hot	3.2%	
					Cool	2.0%	

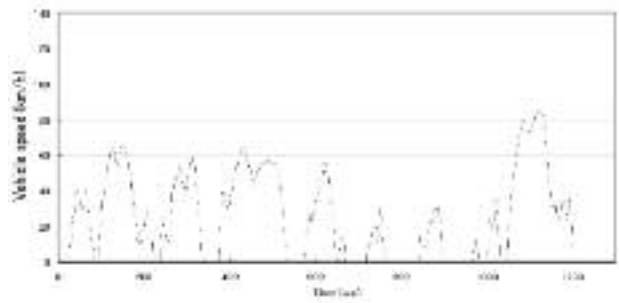


Fig. 13 Japanese JC08 mode drive cycle

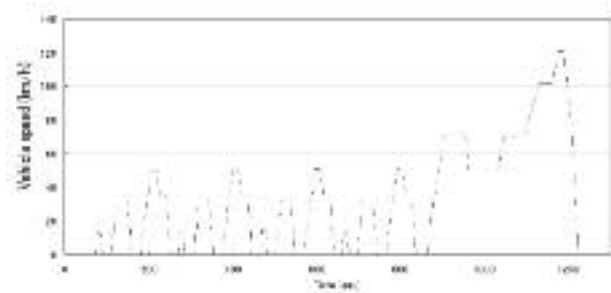


Fig. 14 EURO drive cycle

The results revealed potential improvements to the fuel economy of 2.3% to 8%, varying with drive mode, temperature condition, start condition, and air-conditioning system condition (on/off). Fig. 15 shows a breakdown of braking energy regeneration in each drive mode, measured in hot start test at an outside air temperature of 25°C. Unrecovered energy, accounting for 20% to 30% of the total, corresponds to mechanical losses caused by power transmission paths up to the present system and the planetary gear power transmission. Torque control losses occur when the braking power (regenerative energy) of the system is controlled. More concretely, they are losses caused by the wet electromagnetic brake, accounting for 30% to little less than 50% of the total. FW losses refer to mechanical losses caused by the FW, and motor losses are power generation losses in the

alternator, both of which respectively account for approximately 10%. Remaining energy can be regenerated for use as electricity, which accounts for 20% to 30% of the total braking energy.

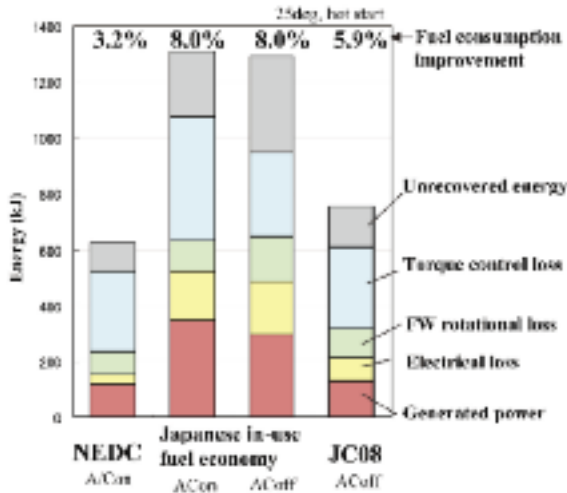


Fig. 15 Recovery energy balance

4. EXPERIMENTAL EVALUATION

A prototype of the system was constructed, installed in a vehicle, and tested in order to quantitatively determine its effects on improving the fuel economy and to identify problems. Fig. 16 shows the structure of the prototype. The aforementioned specifications and structure were modified as shown below due to mounting and temporal restrictions.

① Reduction gear installed on input shaft: The prototype was installed in the large space under the rear seat of a 4WD

vehicle with the vehicle's propeller shaft removed and energy taken from the transfer (see Fig. 17). Accordingly, reduction gear was separately installed to compensate for the insufficient speed increasing ratio of the transfer.

② Use of existing alternator: Since high-speed integrated alternators were under separate assessment, a mass-produced alternator was used and the speed was governed according to the FW speed via reduction gear.

③ Torque control by electric motor: A commercially available AC servomotor was used instead of a dedicated wet electromagnetic brake, since designing it would take time. However, development of a wet electromagnetic brake progressed concurrently. Its responsiveness and other characteristics were simulated by the AC servomotor.

Fig. 18 shows an exterior image of the test vehicle (see Table 4). For good controllability and reproducibility, the test vehicle was placed on test equipment and a dynamo was directly coupled to the front axle to reproduce the load applied to the road surface.

Table 4 Specification of experimental vehicle

models (designation)	TOYOTA PASSO(DBA-KGC35)
Engine	1.0-Liter 3-Cylinder DOHC 4-Valve Variable Valve Timing with intelligence 68hp@6000rpm
Transmission	CVT
Drivetrain	4WD
Weight	920kg
Seating capacity	5

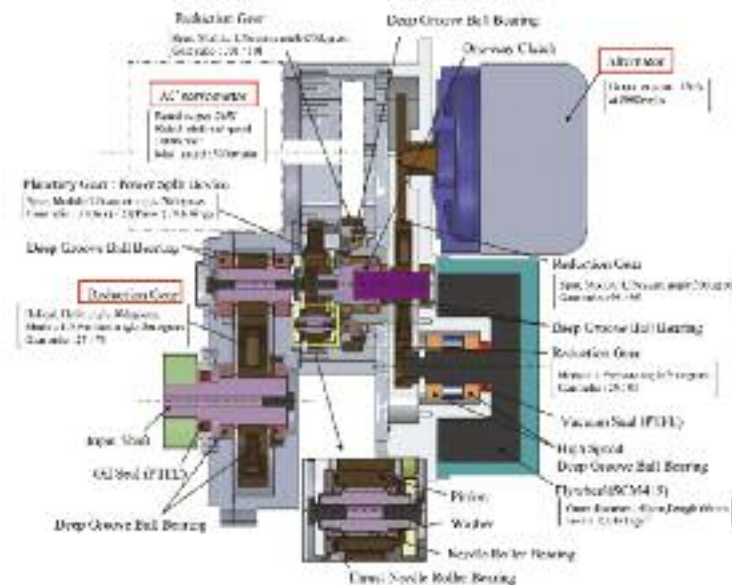


Fig. 16 Structural drawing of trial product



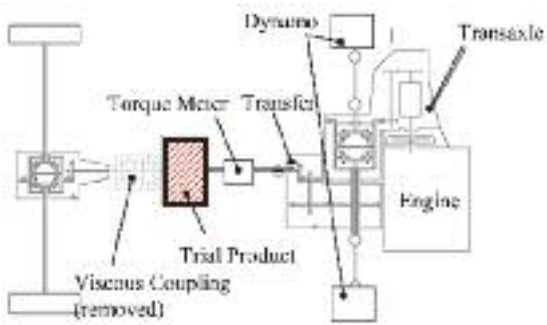


Fig. 17 Schematic of installation place



Fig. 18 Overview of experimental vehicle

Fig. 19 shows braking torque measurement results for the unmounted prototype. While varying the output torque of the AC servomotor coupled to the ring gear of the power split device, braking torque produced on the input and output shafts of the prototype was measured. Fig. 20 shows the mechanical loss measurement results for the FW. It was verified that at the maximum speed of 25000 rpm, the loss was 360 W, approximating the design value.

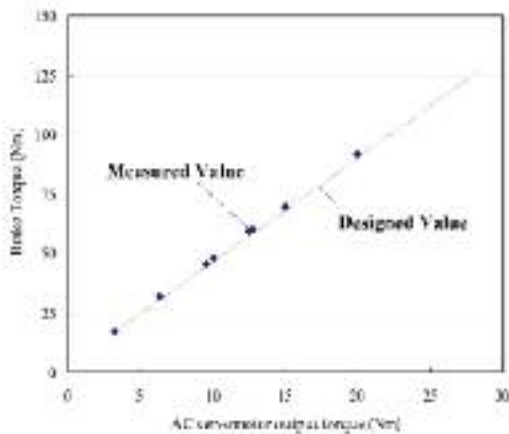


Fig. 19 Brake torque of the trial product

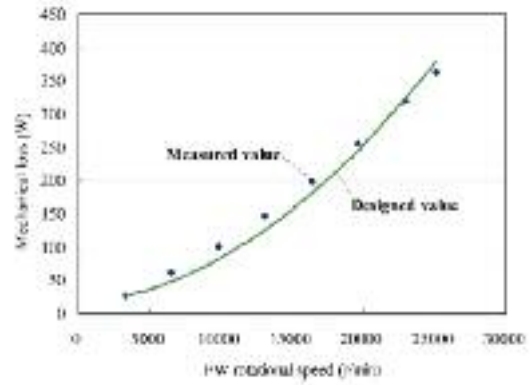


Fig. 20 Flywheel mechanical loss of the trial product

Fig. 21 quantitatively determines the results of fuel economy improvement of the system in in-use fuel economy mode based on the vehicle test results. In contrast to the calculated value, measured effects of the improvement to the fuel economy decreased to 5.5% due to an increase in unrecovered energy (0.8%), increased windage loss (0.3%), and a drag loss increase (1.4%). Fig. 22 compares design and measured regenerative energy values on a time-series basis. The comparison revealed that during driving, light braking was applied by engine braking only (area 1) and that regeneration did not occur in the later deceleration period (area 2).

To regenerate energy dissipated by engine braking, control needs to be implemented to decouple the engine from the axle. In that process, however, the engine speed tends to decrease to the idling speed, probably causing detrimental effects such as a reduced fuel cut time. This is to be analyzed in detail. The cause of area 2 was noise imposed on the rotation signal, which reduced the braking range. This is believed to be solvable.

Regarding windage loss, the operating pressure decreased only to 30 kPa in the vehicle, in contrast to the anticipated pressure of 20 kPa, due to significant resistance caused by the check valve. The drag loss was largely caused by transmission losses occurring upstream of the power split device of the prototype. To solve these problems, we will study additional loss reductions and changing the mounting location of the clutch.

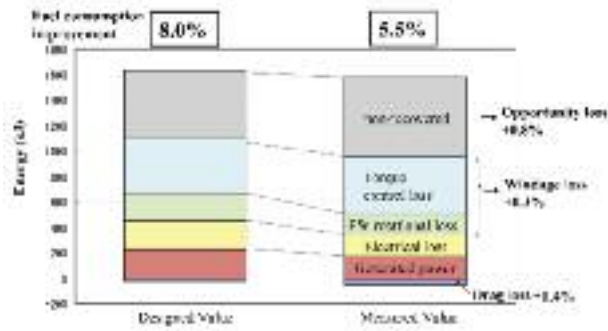


Fig. 21 Fuel consumption improvement

### 5. SUMMARY/CONCLUSIONS

- (1) A simplified mechanical regenerative electricity generation system was designed as a fuel-saving item for conventional cars. The system stores vehicle braking energy simply in the form of kinetic energy and enables use as electricity when needed.
- (2) Calculations and measurements revealed that this system would provide fuel economy improvements of 5.5% (in Japanese in-use mode).
- (3) The following challenges were identified.
  - Engine decoupling control for an increase in the amount of regenerative energy
  - Further reductions in windage, mechanical, and drag losses

We will determine the feasibility of the system, devise solutions for the challenges identified, study other drive modes as well as heat and vibration issues, and work out detailed specifications. As the next step, we will challenge the system, putting the regenerated energy directly back to the drive train.

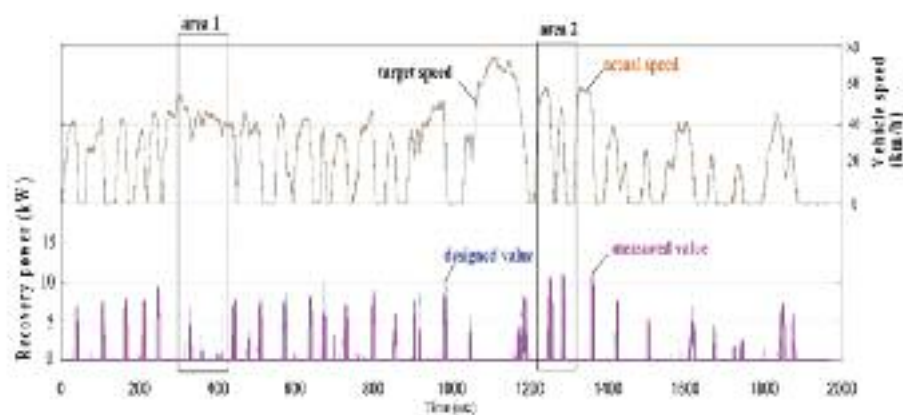


Fig. 22 Braking power

### REFERENCES

- 1) Takefumi Ikui et al., Centrifugal and axial-flow fan compressor, 1960
- 2) O. Zumbusch et al., "Über die Flüssigkeitsreibung umlaufender Scheiben, Zylinder und Zellenkörper" Zeitschrift für Angewandte Mathematik und Mechanik Volume 17, Issue 6, 1937, p356-358
- 3) JSME, Mechanical Engineer's Handbook, B-5, 1987, p18-19
- 4) Japanese Society of Tribologists, Tribology Handbook, 2001, p223-224
- 5) NSK Technical Report, 2007, p166-167

<著 者>



田中 栄太郎  
(たなか えいたろう)  
研究開発2部  
機械系将来製品の開発



成田 隆大  
(なりた たかひろ)  
走行安全事業部  
将来車両システムの開発



前川 仁之  
(まえばわ ひとし)  
日本自動車部品総合研究所  
研究1部  
将来パワトレシステムの研究  
開発